Thermal field formation during wIRA-hyperthermia: temperature measurements in skin and subcutis of piglets as a basis for thermotherapy of superficial tumors and local skin infections caused by thermosensitive microbial pathogens

Piazena, Helmut ; Müller, Werner ; Pendl, Wolfgang ; von Ah, Sereina ; Cap, V H ; Hug, Petra Julia ; Sidler, Xaver ; Pluschke, Gerd ; Vaupel, Peter

Abstract: Purpose: The temporal and spatial formation of the temperature field and its changes during/upon water-filtered infrared-A (wIRA)-irradiation in porcine skin and subcutis were investigated in vivo in order to get a detailed physical basis for thermotherapy of superficial tumors and infections caused by thermosensitive microbial pathogens (e.g., Mycobacterium ulcerans causing Buruli ulcer). Methods: Local wIRA-hyperthermia was performed in 11 anesthetized piglets using 85.0 mW cm-2, 103.2 mW cm-2 and 126.5 mW cm-2, respectively. Invasive temperature measurements were carried out simultaneously in 1-min intervals using eight fiber-optical probes at different tissue depths between 2 and 20 mm, and by an IR thermometer at the skin surface. Results: Tissue temperature distribution depended on incident irradiance, exposure time, tissue depths and individual 'physiologies' of the animals. Temperature maxima were found at depths between 4 and 7 mm, exceeding skin surface temperatures by about 1-2 K. Tissue temperatures above 37 °C, necessary to eradicate M. ulcerans at depths <20 mm, were reached reliably. Conclusions: wIRA-hyperthermia may be considered as a novel therapeutic option for treatment of local skin infections caused by thermosensitive pathogens (e.g., in Buruli ulcer). To ensure temperatures required for heat treatment of superficial tumors deeper than 4 mm, the incident irradiance needed can be controlled either by (a) invasive temperature measurements or (b) control of skin surface temperature and considering possible temperature increases up to 1-2 K in underlying tissue.

DOI: https://doi.org/10.1080/02656736.2019.1655594

tumors and local skin infections caused by thermosensitive microbial pathogens. International Journal of Hyperthermia, 36(1):938-952.
DOI: https://doi.org/10.1080/02656736.2019.1655594

Taylor & Francis
Taylor & Francis Group

International Journal of Hyperthermia

ISSN: 0265-6736 (Print) 1464-5157 (Online) Journal homepage: https://www.tandfonline.com/loi/ihyt20

Thermal field formation during wIRA-hyperthermia: temperature measurements in skin and subcutis of piglets as a basis for thermotherapy of superficial tumors and local skin infections caused by thermosensitive microbial pathogens

Helmut Piazena, Werner Müller, Wolfgang Pendl, Sereina von Ah, Veronika H. Cap, Petra J. Hug, Xaver Sidler, Gerd Pluschke & Peter Vaupel

To cite this article: Helmut Piazena, Werner Müller, Wolfgang Pendl, Sereina von Ah, Veronika H. Cap, Petra J. Hug, Xaver Sidler, Gerd Pluschke & Peter Vaupel (2019) Thermal field formation during wIRA-hyperthermia: temperature measurements in skin and subcutis of piglets as a basis for thermotherapy of superficial tumors and local skin infections caused by thermosensitive microbial pathogens, International Journal of Hyperthermia, 36:1, 937-951, DOI: 10.1080/02656736.2019.1655594

To link to this article: https://doi.org/10.1080/02656736.2019.1655594

INTERNATIONAL JOURNAL OF HYPERTHERMIA
2019, VOL. 36, NO. 1, 937–951
https://doi.org/10.1080/02656736.2019.1655594

Thermal field formation during wIRA-hyperthermia: temperature measurements in skin and subcutis of piglets as a basis for thermotherapy of superficial tumors and local skin infections caused by thermosensitive microbial pathogens

Helmut Piazena[a], Werner Müller[b], Wolfgang Pendl[c], Sereina von Ah[c], Veronika H. Cap[d], Petra J. Hug[d], Xaver Sidler[c], Gerd Pluschke[e] and Peter Vaupel[f]

[a]Medical Photobiology Group, Department of Internal Medicine, Charité-University Medicine Berlin, Berlin, Germany; [b]Physical Optics Consultant Office, Wetzlar, Germany; [c]Department of Farm Animals, Division of Swine Medicine, Vetsuisse Faculty, University of Zürich, Zürich, Switzerland; [d]Section of Anaesthesiology, Equine Department, Vetsuisse Faculty, University of Zürich, Zürich, Switzerland; [e]Department of Medical Parasitology and Infection Biology, Molecular Immunology Unit, Swiss Tropical and Public Health Institute, Basel, Switzerland; [f]Department of Radiation Oncology, University Medical Center, Freiburg i. Breisgau, Germany

ABSTRACT

Purpose: The temporal and spatial formation of the temperature field and its changes during/upon water-filtered infrared-A (wIRA)-irradiation in porcine skin and subcutis were investigated in vivo in order to get a detailed physical basis for thermotherapy of superficial tumors and infections caused by thermosensitive microbial pathogens (e.g., *Mycobacterium ulcerans* causing Buruli ulcer).

Methods: Local wIRA-hyperthermia was performed in 11 anesthetized piglets using 85.0 mW cm^{-2}, 103.2 mW cm^{-2} and 126.5 mW cm^{-2}, respectively. Invasive temperature measurements were carried out simultaneously in 1-min intervals using eight fiber-optical probes at different tissue depths between 2 and 20 mm, and by an IR thermometer at the skin surface.

Results: Tissue temperature distribution depended on incident irradiance, exposure time, tissue depths and individual 'physiologies' of the animals. Temperature maxima were found at depths between 4 and 7 mm, exceeding skin surface temperatures by about 1–2 K. Tissue temperatures above 37 °C, necessary to eradicate *M. ulcerans* at depths <20 mm, were reached reliably.

Conclusions: wIRA-hyperthermia may be considered as a novel therapeutic option for treatment of local skin infections caused by thermosensitive pathogens (e.g., in Buruli ulcer). To ensure temperatures required for heat treatment of superficial tumors deeper than 4 mm, the incident irradiance needed can be controlled either by (a) invasive temperature measurements or (b) control of skin surface temperature and considering possible temperature increases up to 1–2 K in underlying tissue.

ARTICLE HISTORY
Received 15 May 2019
Revised 5 August 2019
Accepted 7 August 2019

KEYWORDS
Water-filtered infrared-A (wIRA-) hyperthermia; superficial hyperthermia; invasive temperature measurement; heat treatment of thermosensitive pathogens; hyperthermia of superficial tumors

1. Introduction

Water-filtered infrared-A (wIRA) radiation (780–1400 nm) [1] shows a significantly deeper penetration into skin and subcutaneous tissue compared to unfiltered IR-A radiation and both, the middle (IR-B, 1400–3000 nm) and the long-wavelength (IR-C, 3000 nm–1 mm) infrared radiation [2,3]. This property causes basic differences concerning tissue heating as compared to conventional heat sources used in thermotherapy such as unfiltered IR-A, IR-B, IR-C, heating packs, hot-water baths and heated air/vapor flows reported by various authors. Advantages include (a) significant heat generation by absorption of radiation not only in the uppermost skin layers or at the skin surface, but also in deeper tissues layers [3]; (b) threshold skin surface temperatures for induction of heat pain [4,5] are reached at significantly higher incident irradiances as compared to short-wavelength IR (by a factor of about 2.5) and IR-C (by a factor of about 3.6) [2,6] and (c) significantly smaller temperature decrease within deeper tissue layers as compared to short-wavelength IR or hot packs [7].

During the past three decades, superficial wIRA-hyperthermia (wIRA-HT) attained growing interest in dermatology, regenerative medicine, neurology [8] and also in (adjuvant) cancer treatment [9–22] using local, contact-free, superficial hyperthermia (39–43 °C) or whole-body hyperthermia (WBH) with temperatures of 38.5–40.5 °C in moderate ('fever range') WBH, and 40.5–42.0 °C in 'extreme' WBH. Recently, Notter et al. reported promising data showing the efficacy of wIRA-HT in the treatment of large-sized recurrent breast cancer [23,24]. Piazena et al. [6] and Vaupel et al. [25] provided related physical and photobiological basics with reference to the ESHO quality assurance guidelines for superficial hyperthermia in oncology [26,27].

CONTACT Helmut Piazena helmut.piazena@charite.de Department of Internal Medicine, Medical Photobiology Group, Charité-University Medicine Berlin, Charité-Platz 1, 10117 Berlin, Germany

Supplemental data for this article is available online at on the publisher's website.

New perspectives for thermal therapy to treat infectious diseases and to eliminate a number of thermosensitive pathogens in vivo were recently discussed by Gazel and Yilmaz [28]. In this context, wIRA-hyperthermia could be a useful alternative/adjuvant ('thermal-microbiology concept' [28]) to antibiotic (e.g., Rifamycine and Streptomycine) and surgical measures [29,30] as well as to the application of jackets filled with heated water [31] or of chemical (exothermal) phase change material packs [32] for local treatment of, for example, Buruli ulcers, frequent infections in tropical and subtropical countries [33].

Respective therapeutic interventions use skin surface temperatures of about 40 °C in the ulcerated area for several hours per day for about 2 months. Temperatures above 37 °C are needed to inactivate and eliminate the pathogen in the infected tissue [31,32,34]. According to Ruf et al. [35] the causative thermosensitive pathogen *Mycobacterium ulcerans* is located at depths in the tissue up to about 13 mm. In contrast to the sole thermally based treatment [28–35], Kuratli et al. [36] have described nonthermal reduction of *chlamydial* infectivity by wIRA in combination with visible radiation. This thermotherapeutic concept, that is, eradication of thermosensitive bacteria by hyperthermia, has been described in detail recently [37–43].

Whereas thermotherapy should be effective to ensure the therapeutic goal, it should also avoid unintentional thermal injury of the exposed tissue due to overheating using temperatures above about 43 °C for too long exposure times [4,44–46]. In most cases it is inconvenient to directly assess the tissue temperatures therapeutically required during the treatment by invasive measurements. Instead, heat pain response by the patient or temperature measurements on the skin surface are commonly used to estimate the actual heat impact within the target region. However, it is well known that tissue burns may occur during IR therapy even if the skin surface temperature remains below the heat pain threshold, an effect which depends on the individual ability for heat dissipation in the irradiated tissues.

Heat dissipation is determined by the thickness of the subcutaneous fat layer, the body core temperature and the effectiveness of both, conductive (by molecular movements) and convective (by blood flow) heat transport. Thus, only in the case of defined and known relationships between tissue temperature and skin surface temperature, assessment of the latter is sufficient. Therefore, using a porcine model, an excellent animal model for the profiling of this new therapeutic intervention [47], as a first step before starting systematic investigations in humans, two goals of this preclinical in vivo study were defined: (a) determination of the interrelation between the skin surface temperature and the tissue temperature upon wIRA-irradiation and its individual variability, and (b) assessment of the relationship between the temperature depth profile and the kinetics of tissue heating as a function of irradiance, exposure time and individual factors affecting heating (e.g., thickness of the skin and of the fat layer, body core temperature and efficacy of thermoregulation). Key parameters of the current evaluation were (a) heating-up times to reach target temperatures between 39 °C and 43 °C up to depths of 20 mm within the tissue, (b) maximum and mean temperatures and their deviations as a function of tissue depth and (c) persistence of tissue temperatures and thermal skin erythema after wIRA-heating. Experiments were performed using a diameter of the exposed skin area ≥10 cm for skin and subcutis heating which is representative for both, large-size ('loco-regional') skin IR-irradiation [48] as used in localized hyperthermia and whole body IR-irradiation before the onset of systemic heat regulation (e.g., by sweating).

2. Material and methods

2.1. Animals

Eleven piglets were incorporated in the study (body weights 15–25 kg). Before treatment, skin hairs were sheared within the target area, then the skin was cleaned, and the thicknesses of skin and fat layers were measured with an ultrasound scanner (type: HS-166V with probe No. HCS-8712M/7.5 MHz, Honda Electronics, Toyohashi, Japan).

Animals were divided by random sampling into three groups for three different incident irradiances (see Table 1) and were anesthetized using the following protocol: after sedation with ketamine (10 mg kg^{-1} i.m.) and medetomidine (50 μg kg^{-1} i.m.), general anesthesia was induced with propofol i.v. until anesthetic depth allowed intubation. Anesthesia was maintained with sevoflurane (end-tidal 3%). The piglets were ventilated to keep respiratory parameters constant (inspiratory O_2 concentration: 40 ± 5%, and end-tidal CO_2 partial pressure: 45 ± 5 mmHg), and were infused with a balanced infusion solution (Ringer's lactate: 5 ml kg^{-1} h^{-1}) in order to keep mean arterial blood pressure >50 mm Hg. Before treatment the body core temperatures of the animals varied between 37.7 °C and 39.0 °C, and ranged between 38.3 °C and 39.0 °C upon treatment.

2.2. wIRA-irradiation

As shown in Table 1, three different incident irradiances were achieved by distance variation between the exit window of the irradiator and the skin surface (37, 42 and 47 cm) in order to exclude changes of the incident wIRA-spectrum. Verification measurements were performed using a double-

Table 1. Individual thicknesses of skin and fat layers, and body core temperature before and immediately after wIRA-irradiation of piglets p2–p12, divided into three groups according to the different irradiances (IR-A) applied.

Piglet	Irradiance (IR-A) (mW cm^{-2})	Thickness (mm) of		Body core temperature (°C)	
		Skin	Fat layer	Before	After
p2	126.5	5.0	5.0	39.0	39.0
p3		5.0	5.0	37.7	38.8
p4		1.0	3.2	38.2	38.7
p5		5.0	6.0	38.3	38.5
p6	103.2	4.3	5.0	38.2	38.7
p7		4.5	5.5	38.1	39.0
p8		3.8	5.5	38.2	38.8
p9		4.9	4.1	38.2	38.9
p10	85.0	3.8	4.4	38.1	38.8
p11		4.9	5.2	38.0	38.3
p12		3.8	4.9	37.8	38.4

monochromator spectroradiometer (type SPECTRO 320D, Instrument Systems, Munich, Germany). Before starting the study, the spectroradiometer was calibrated by the manufacturer, whereas offset correction was performed before each measurement. Measured spectra of irradiance are shown in Figure 1. Irradiance data were calculated by integrating the spectral irradiance data over the wavelength within the respective spectral subranges (shown in Table 2). According to these data, about 73% of the total irradiance came from the IR-A range. During the measurements, both the exit window of the irradiator and the Ulbricht sphere used as entrance window of the spectroradiometer were parallel and centered to each other.

2.3. Temperature measurements

Tissue temperatures were measured simultaneously in 1-min intervals within the treated area before, during and after wIRA-irradiation with an IR thermometer at the skin surface (type FLUKE 575, FLUKE, Everett, USA) and with eight fiber-optical probes vertically inserted into the tissue at depths of 2, 4, 7, 8, 10, 12, 16 and 20 mm (type: PSC-D-N-N-N with 8 Opsens-ProSensModul PSR-G1-N-100ST-L and probe type: OTG-M600-10-62ST-3.OPTFE-XN-00PIT-M1, Soliton Laser- und Messtechnik, Gilching, Germany). The sheathing at the end of the probes was stripped according to the desired depths (tip diameter: 0.5 mm). Before measurements, the probes were calibrated in ice water. In this way, the relative error of the probes was limited to ±0.3 K. According to the manufacturer's information, resolution of the probes is 0.03 K, and the response time 10 ms.

The accuracy of the infrared thermometer was verified by comparison to the readings of a precision mercury thermometer immersed into homogeneously tempered water. Temperatures of the infrared thermometer measured at the water surface differed by less than ±1.5% within the range of 30–50 °C. For this test, the infrared thermometer was used with an emission coefficient of $\varepsilon \approx 0.93$, and was set to $\varepsilon \approx 0.98$ for skin temperature measurements.

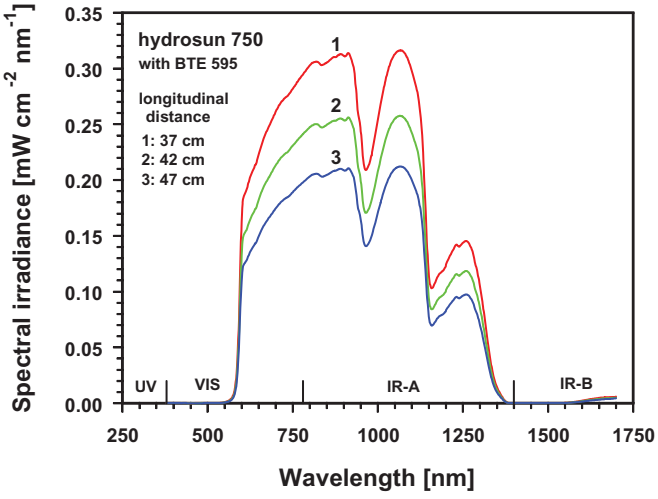

Figure 1. Spectral irradiance of the wIRA irradiator as a function of wavelength [irradiator type: hydrosun 750 (hydrosun, Müllheim, Germany), equipped with a cutoff filter (type BTE 595, BTE Elsoff, Germany)]. Measurements were performed at longitudinal distances of 37 cm (curve 1), of 42 cm (curve 2) and of 47 cm (curve 3) between the center of the exit window of the irradiator and the center of the radiation entrance window of the spectroradiometer. Both windows were parallel to each other.

Table 2. Incident irradiance in the spectral range of IR-A (780–1400 nm), in the 'total' spectral range of spectroradiometric measurement (380–1700 nm) and in the ranges of VIS_1 (380–590 nm), of VIS_2 + IR-A (590–1400 nm) and of IR-B* (1400–1700 nm) as part of the spectral range of IR-B (1400–3000 nm) in the center of the irradiated skin area as a function of longitudinal distances between this area and the exit window of the irradiator.

	Irradiance (mW cm^{-2}) in the spectral range of				
Longitudinal distance (cm)	IR-A	'Total'	VIS_1	VIS_2 + IRA	IR-B*
37	126.525	173.104	0.455	172.112	0.545
42	103.200	141.246	0.372	140.427	0.453
47	84.975	116.209	0.308	115.524	0.382

2.4. Assessment of skin redness

Skin redness was recorded to assess changes in peripheral blood flow/blood volume before and after exposure with a spectrophotometer type SPECTROPEN (Dr. Lange, Düsseldorf, Germany) which differentiates object colors into the components red-green (a*), blue-yellow (b*) and light-dark (L*) according to CIE [49]. The spectrophotometer was calibrated before each experiment with a white reflectance standard (type: SRS-99-010 AQS-01160-060, S/N OC55C-1537, Labsphere, North Sutton, NH, USA).

2.5. General procedures

Each piglet was exposed only once choosing an incident irradiance according to Table 1. Treatments were performed on a special table in an operating room of the Animal Hospital of the University of Zürich, Switzerland. Body-core temperatures (in the esophagus) and vital functions of the animals were monitored continuously during wIRA-irradiation. Room air temperature was between 22 °C and 24 °C (no air flow, monitoring of humidity).

wIRA-irradiation was focused on a circular area (10 cm diameter) at the upper left thigh, which was nearly planar (deviations from ideal planarity ≤1 cm) and centric to the radiation exit window of the irradiator. According to Figure 2, there was only a deviation of ≤0.47% from an ideal homogeneity of irradiance within the target area. The angle between the beam and the skin surface was orthogonal (Figure 3).

wIRA-treatments were carried out for a maximum of 60 min, or until a thermal steady state was reached. The irradiation was terminated when temperatures reached 45 °C, that is, the threshold level for possible burns according to DIN 33403/2 [5]. After completion of wIRA-exposure, temperature measurements were continued until the baseline values before irradiation were reached again. When symptoms of the end of anesthesia became obvious, temperature measurements were also stopped.

3. Results and discussion

3.1. Individual thermal responses to wIRA-irradiation

The complete documentation of surface and tissue temperature data sets measured as a function of time and depth before, during and after wIRA-irradiation of each piglet is presented in the Supplemental Material.

Measured temperatures showed significant individual differences during wIRA-irradiation. This is exemplarily shown for four piglets in Figures 4a–d and 5a–d. Table 3 provides related relevant temperatures and a characterization of thermal responses for different layers of the heated tissue.

Two of these piglets (p2 and p3) were exposed to the same wIRA-irradiance (126 mW cm^{-2}). However, in p2 there was a continuous temperature rise (heat accumulation) in all tissue layers, exceeding the threshold for burns in the skin and in the upper fat layer (Figure 4d). In contrast, p3 reacted with an effective thermoregulation which resulted in a temperature maximum of 43.6 °C at the skin surface and in lower temperatures within the underlying tissue (see Figure 4a).

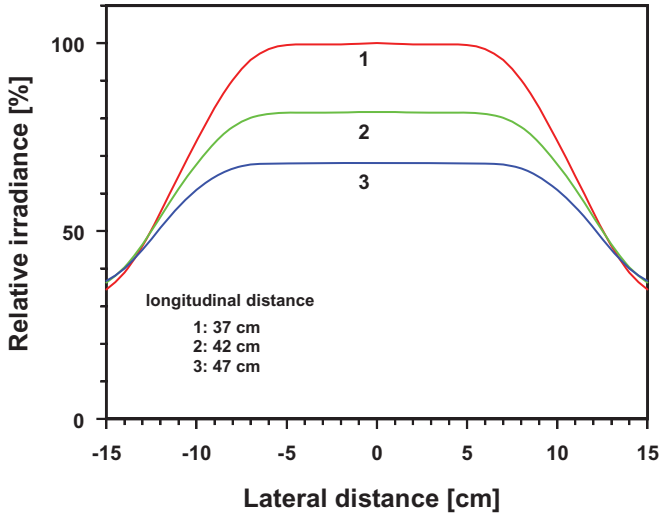

Figure 2. Relative irradiance (%) as a function of the lateral distance to the center, normalized to the value measured at the center of the exposed/irradiated area at longitudinal distances of 37, 42 and 47 cm.

Piglets p6 and p10 could regulate their tissue temperatures; however, with different kinetics and extents compared to p3 (Figure 4b–c). Temperature maxima upon wIRA-irradiation were observed within the tissue for both piglets, but not at the skin surface (Figure 4b–c). Moreover, minor irradiance in p10 resulted in a more homogeneous but lower tissue heating (as compared to p2 and p3) and in an earlier final thermal steady state (as compared to p3 and p6).

More details are illustrated in Figures 4a–d and 5a–d showing individual responses depending on incident irradiance, exposure time, thicknesses of skin and fat layer, tissue depths and individual ability for heat dissipation within the tissue by conduction and convection. The body core temperature increased only marginally from 38.0 to 38.5 °C for p3, p6 and p10, or remained almost constant at 39.0 °C for p2 (curves 10). Because of this complexity, the interrelation between all these influencing factors needs to be analyzed in more detail as outlined in the following.

3.2. Effects of wIRA-irradiation within the different groups

From Figures 4d and 5d it is obvious that piglet p2 most probably is an outlier due to higher body core temperature and inability for effective thermoregulation. Therefore, analyses of mean thermal responses in group 1 were performed without considering the temperature data of p2 in Figures 6–10.

3.2.1. Tissue temperatures as a function of irradiation time

Temperatures at different tissue depths (means and standard deviations) as a function of irradiation time are shown in Figures 6a–d and 7a–d. Table 4 provides a summary of means and standard deviations of the maximum temperatures and the thermal steady-state temperatures (SST) for different tissue depths. Temperature maxima during the wIRA-irradiation differed in the tissue on average by 2.1 K in group 1 (exposed to 126.5 mW cm^{-2}) and by only 1.1 K in group 2 (103.2 mW cm^{-2}) and group 3 (85.0 mW cm^{-2}) which

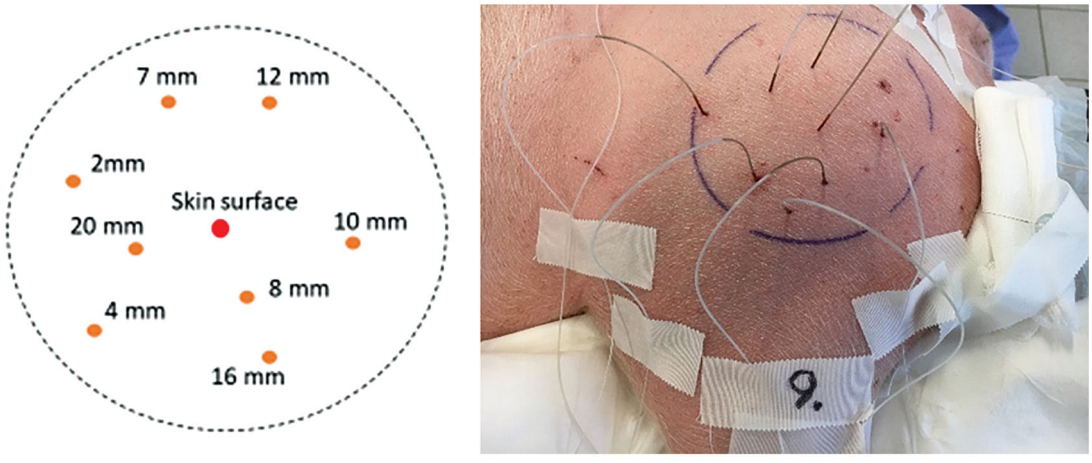

Figure 3. Template for sensor positions and indication of depths at which temperature measurements were performed (left), marked target field with inserted temperature sensors (right). The sensors were inserted with the aid of catheters (Type SURFLO IV Catheter and SUPERFLASH IV Catheter, TERMURO, Tokyo, Japan).

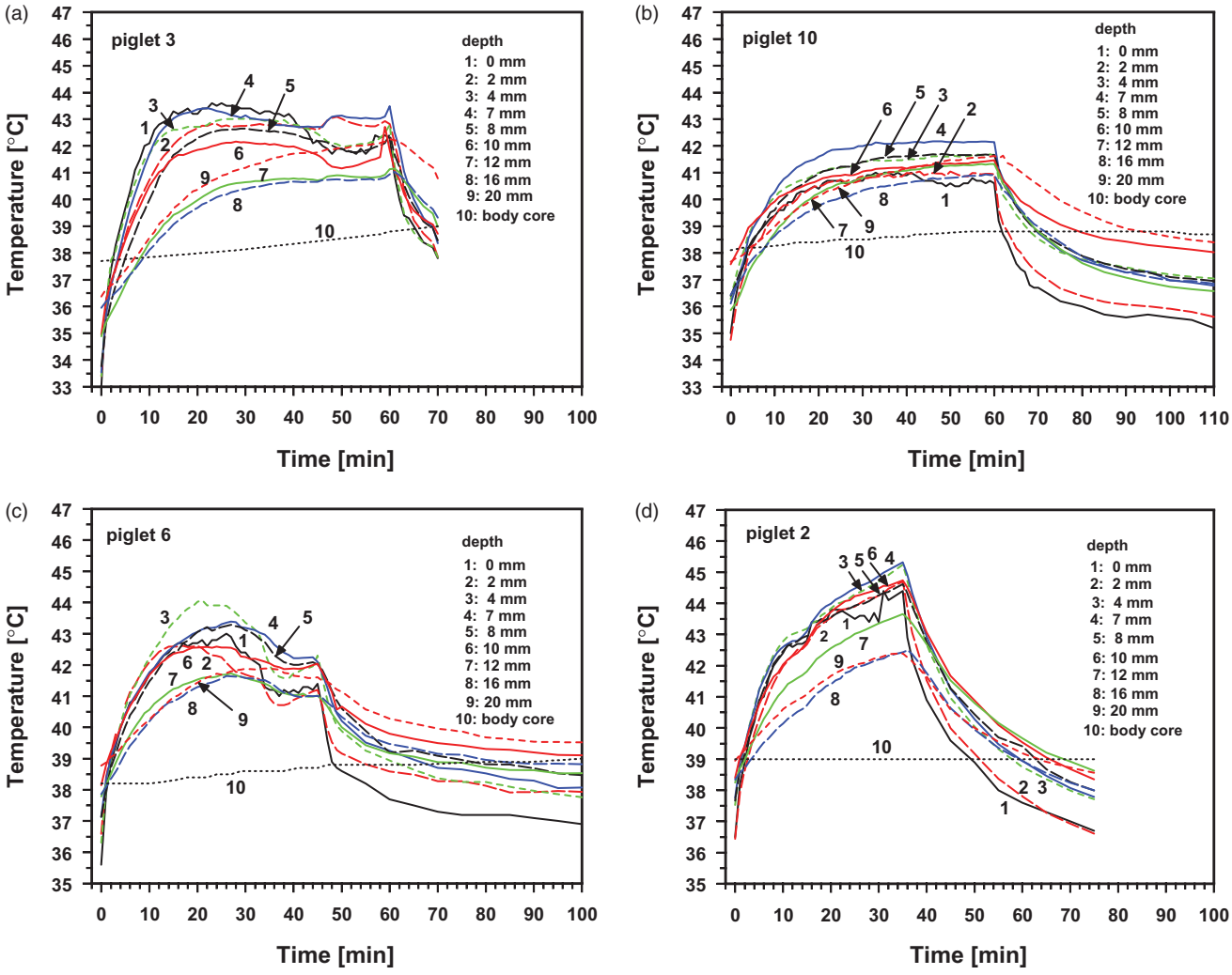

Figure 4. Surface temperature (curve 1), tissue temperatures at depths of 2–20 mm (curves 2–9) and body core temperature (curve 10) of selected piglets during and after wIRA-irradiation as a function of time. The following incident irradiances (IR-A) were chosen: 126.5 mW cm^{-2} (a: p3, d: p2), 103.2 mW cm^{-2} (c: p6) and 85.0 mW cm^{-2} (b: p10).

indicates a more homogeneous heating of the tissue in the latter groups as compared to group 1. SST was observed only in groups 2 and 3 at all depths, whereas it was not observed at the skin surface and in the deeper part of the fat layer in group 1.

3.2.2. Initial temperature increase and the onset of local thermoregulation in the skin

Immediately after starting wIRA-irradiation, a rapid temperature rise was observed depending on the incident irradiance and the tissue depth. All piglets reacted by initiating local thermoregulation in the skin. Thermal steady states were reached after about 20–30 min. However, intermediate thermal responses showed two main characteristics: (a) striking deviances of the standard deviations of the temperatures from their respective means as depicted in Figures 6a–d and 7a–d. This was observed even for the *same* irradiance applied within the groups indicating significant differences in the individual processes of heat dissipation in terms of onset time and extent of increased peripheral perfusion, and (b) occurrence of temporary temperature maxima at the skin surface and in the skin before the onset of an effective temperature down-regulation in the case of higher irradiances. This phenomenon was observed in groups 1 and 2 (exposed to IR-A of 126.5 and 103.2 mW cm^{-2}, respectively; see Figures 6a–c, curves 1 and 2) whereas the skin surface temperature and the temperature within the skin increased continuously up to thermal steady states in group 3 (exposed to 85 mW cm^{-2}, see Figures 6a–c, curve 3).

3.2.3. Impact of the fat layer

Due to radiation absorption mainly in the skin [2,3,6,7] and due to the insulating properties of the fat layer, rapid temperature increases, heat accumulation and temperature decrease by local thermoregulation occurred mainly above the fat layer. Moreover, the predominant conductive heat transport from the skin surface to deeper tissues and the ineffective heat dissipation in the fat layer caused (with varying delays) temperature rises with increasing depth in tissues underlaying the skin. Therefore, temperature profiles in the upper part of the fat layer (at a depth of 7 mm) were similar, but less pronounced than in the skin (see Figure 6d),

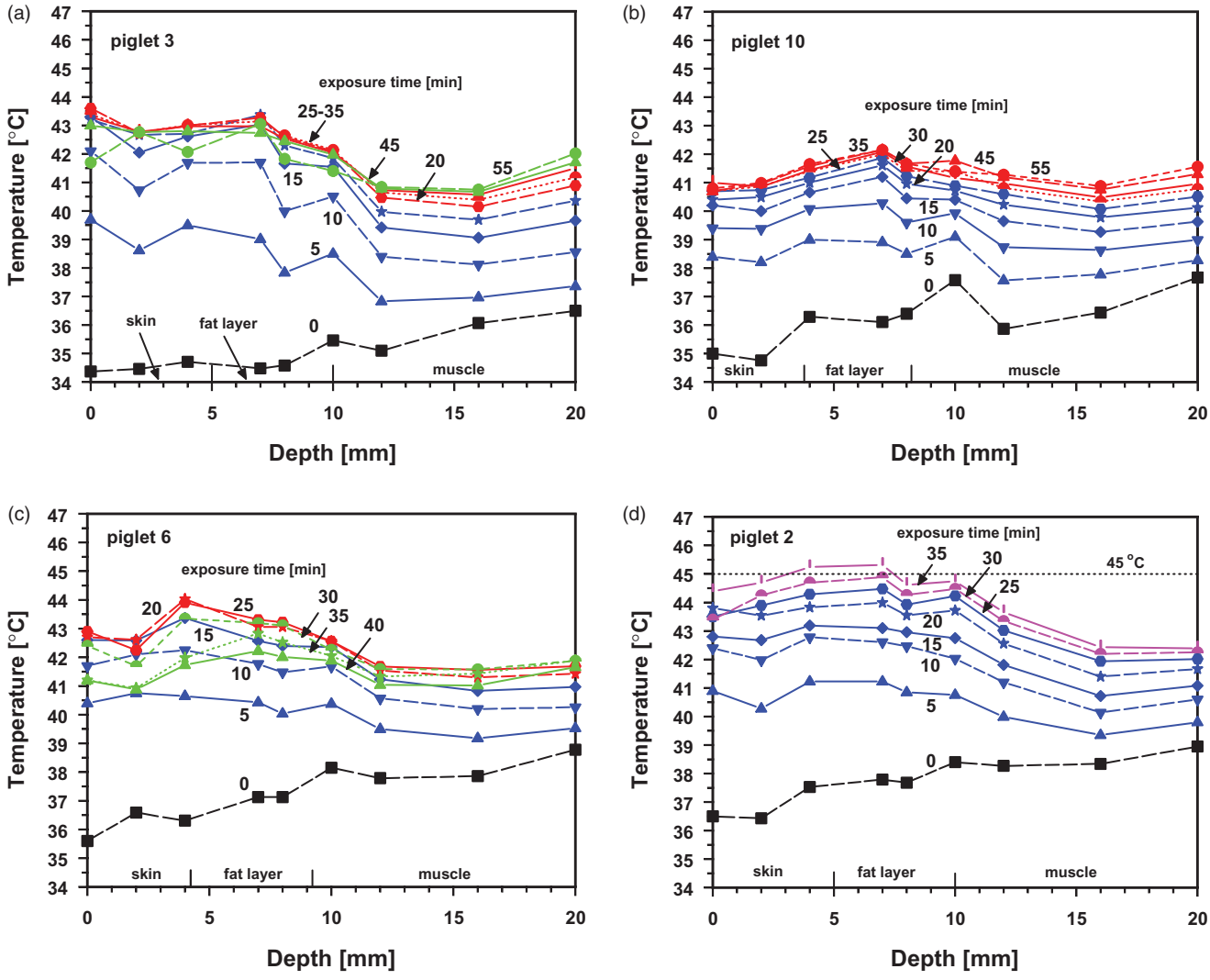

Figure 5. Tissue temperature of piglets p2 and p3 [d and a, exposed to wIRA with 126.5 mW cm^{-2} (IR-A)], of piglet p10 [b, exposed to 85.0 mW cm^{-2} (IR-A)] and of piglet p6 [c, exposed to 103.2 mW cm^{-2} (IR-A)] as a function of tissue depth before (curves 0) and during various irradiation at times.

whereas tissue temperatures increased (continuously, but somewhat delayed) to mean SST of 42.1–42.4 °C in the deeper part of the fat layer (at a depth of 10 mm) and of 41.1–41.5 °C in the subcutis at depths between 12 and 20 mm (see Figures 7a–d).

3.2.4. Temperature differences between skin surface and tissue

According to the data shown in Table 4, temperatures in the upper layers of the tissue exceeded the temperatures at the skin surface in all animals. This most probably is caused by (a) heat accumulation in the tissue above the fat layer, (b) decreased heat transfer into the subcutis due to the insulating fat layer and (c) heat transfer from the skin surface to the environment.

3.2.5. Vertical temperature profiles

The baseline tissue temperatures before wIRA-irradiation increased continuously from the skin surface to deeper tissue layers (curves 0 and black symbols in Figures 8a–d). wIRA-irradiation resulted in the following characteristic effects (curves 1–3 in Figures 8a–d): (a) temperature maxima within in the skin at a depth of 4 mm were observed immediately after starting wIRA-irradiation, persisting during the whole irradiation period; (b) mean temperatures increased with higher irradiance and longer exposure time and (c) enlarging differences between the maximum temperature in the tissue and at the skin surface with increasing exposure time. Notably, the depth profile of group 2 (medium irradiance) was similar to the profile of group 1 (high irradiance) after 5 min of exposure, whereas it resembled the profile of group 3 (low irradiance) after 30 min, obviously initiated by effective thermoregulation in the animals of group 2 (see Figures 8a–d). This phenomenon could be of interest for scheduling of therapeutic hyperthermia when mild tissue heating with low irradiances is needed.

3.2.6. Impact of individual deviations from mean hyperthermia temperatures

wIRA-irradiation can individually result in (unintentional) lower or higher tissue temperatures compared to the mean data in Table 4, and as documented in Figures 6–8.

Table 3. Phases of temperature response upon wIRA-irradiation.

Piglet	Tissue	T_0 (°C)	Phases of temperature response	T_{max} (°C)	T_{min} (°C)	Related figures
p3	Skin surface	33.0	(I) Initial increase	43.6	41.7	4a, curve 1
irradiance:	Skin	33.4	(II) Nearly constant (SST)	43.0	41.9	4a, curves 2 and 3
126.5			(III) Decrease due to LTR			
mW cm^{-2}	Fat layer (o.p.)	33.5	(I) Initial increase to maximum	43.4	42.7	4a, curve 4
skin:			(II) Decrease to SST due to LTR in the skin			
5.0 mm	Fat layer (i.p.)	34.9	(I) Initial increase	42.6	41.2	4a, curves 5 and 6
fat layer:			(II) Nearly constant (SST)			
5.0 mm			(III) Decrease to SST due to LTR in the skin			
	Subcutis	36.7	(I) Initial increase to maximum	41.9	–	4a, curves 7–9
			(II) Nearly constant (SST)			
p2	Skin surface	36.4	Continuous increase to maximum (no LTR, no thermal steady state)	44.4	–	4d, curve 1
irradiance:	Skin	37.5		45.3	–	4d, curves 2 and 3
126.5	Fat layer (o.p.)	37.8		45.3	–	4d, curve 4
mW cm^{-2}	Fat layer (i.p.)	38.4		44.6	–	4d, curves 5 and 6
skin:	Subcutis	39.0		43.6	–	4d, curves 7–9
5.0 mm						
fat layer:						
5.0 mm						
p6	Skin surface	35.6	(I) Initial increase	43.0	41.1	4c, curve 1
irradiance:	Skin	36.6	(II) Decrease due to LTR in the skin	44.0	41.6	4c, curves 2 and 3
103.25	Fat layer (o.p.)	37.1	(III) Nearly constant at minimum (SST)	43.4	42.3	4c, curve 4
mW cm^{-2}	Fat layer (i.p.)	38.2		43.3	41.9	4c, curves 5 and 6
skin:	Subcutis	38.8		41.6	41.0	4c, curves 7–9
4.3 mm						
fat layer:						
5.0 mm						
p10	Skin surface	34.0	(I) Initial increase	41.0	40.4	4b, curve 1
irradiance:	Skin (o.p.)	34.8	(II) Nearly constant (SST)	41.0	40.8	4b, curve 2
85.0			(III) Decrease due to LTR			
mW cm^{-2}	Skin (i.p.)	36.3	(I) Initial increase to maximum	41.7	–	4b, curve 3
skin:	Fat layer (o.p.)	36.1	(II) Nearly constant at maximum (SST)	42.1	–	4b, curve 4
3.8 mm	Fat layer (i.p.)	37.6		41.5	–	4b, curves 5 and 6
fat layer:	Subcutis	37.7	Continuous increase to maximum	41.5	–	4b, curves 7–9
4.4 mm						

Baseline temperatures before (T_0), maximum (T_{max}) and minimum temperatures (T_{min}) during wIRA exposure at the skin surface and in various tissue layers of selected piglets.
SST: thermal steady state temperature; LTR: local thermoregulation; o.p.: outer part; i.p.: inner part.

Using the data of Figures 8a–d, two criteria were evaluated to estimate possibly lower deviations assuming normal distributions of reached tissue temperatures with wIRA-irradiation in the piglets:

- The temperature at the lower limit of the standard deviation:

$$T_{\sigma l} = T_{mean} - \sigma \quad (1)$$

- The temperature at the lower confidence limit of the mean using a significance level of 5%:

$$T_{lcl} = T_{mean} - (\sigma \times t/\sqrt{n}) \quad (2)$$

(T_{mean}: mean temperature, σ: standard deviation, n: number of piglets, t: critical value of Student's t-distribution ($t = 4.30$ for $n = 3$, groups 1 and 3 and $t = 3.18$ for $n = 4$, group 2) [50].

According to these conditions, tissue temperatures $\leq T_{\sigma l}$ may be expected in about 16%, and temperatures $\leq T_{lcl}$ in about 2.5% of all cases. This results in decreased depths of tissue layers which can be heated up to therapeutically required temperature levels as shown in Table 5 for irradiation times of 30 min. Irradiation times <20–30 min are too short to generate thermal steady states. (For more details see Figures S13a–d and S14a–d in the Supplemental Material.)

As shown in Figures 4d, 5d, 6c, 8d and 11, unintentional hot spots in the tissue with temperatures up to about 45 °C were observed in single cases after exposure times of 20–30 min. As stated earlier [44–46], these temperature maxima may be sufficient to cause irreversible epidermal injury and skin burning in both porcine and human skin if critical exposure times were exceeded. Therefore, hyperthermia using wIRA and treatment times ≥30 min requires additional measures of heating control to ensure both, the therapeutic success and the prevention of possible thermal injury and tissue burns.

3.2.7. Correlation between surface and tissue temperature during wIRA-irradiation

Skin surface temperatures are often used to control hyperthermia instead of (more complex) invasive temperature measurements. For safety reasons, when surface temperature measurements are used, it is mandatory to consider the formation of temperature maxima that may occur within the tissue. Therefore, a comparison between synchronous maximum temperatures at the skin surface and in the tissue is shown for each piglet in Figure 11a. According to these data, the maximum tissue temperature can exceed the skin surface temperature by about 1 K in most cases and can reach about 2 K in some piglets. The differences of the temperature

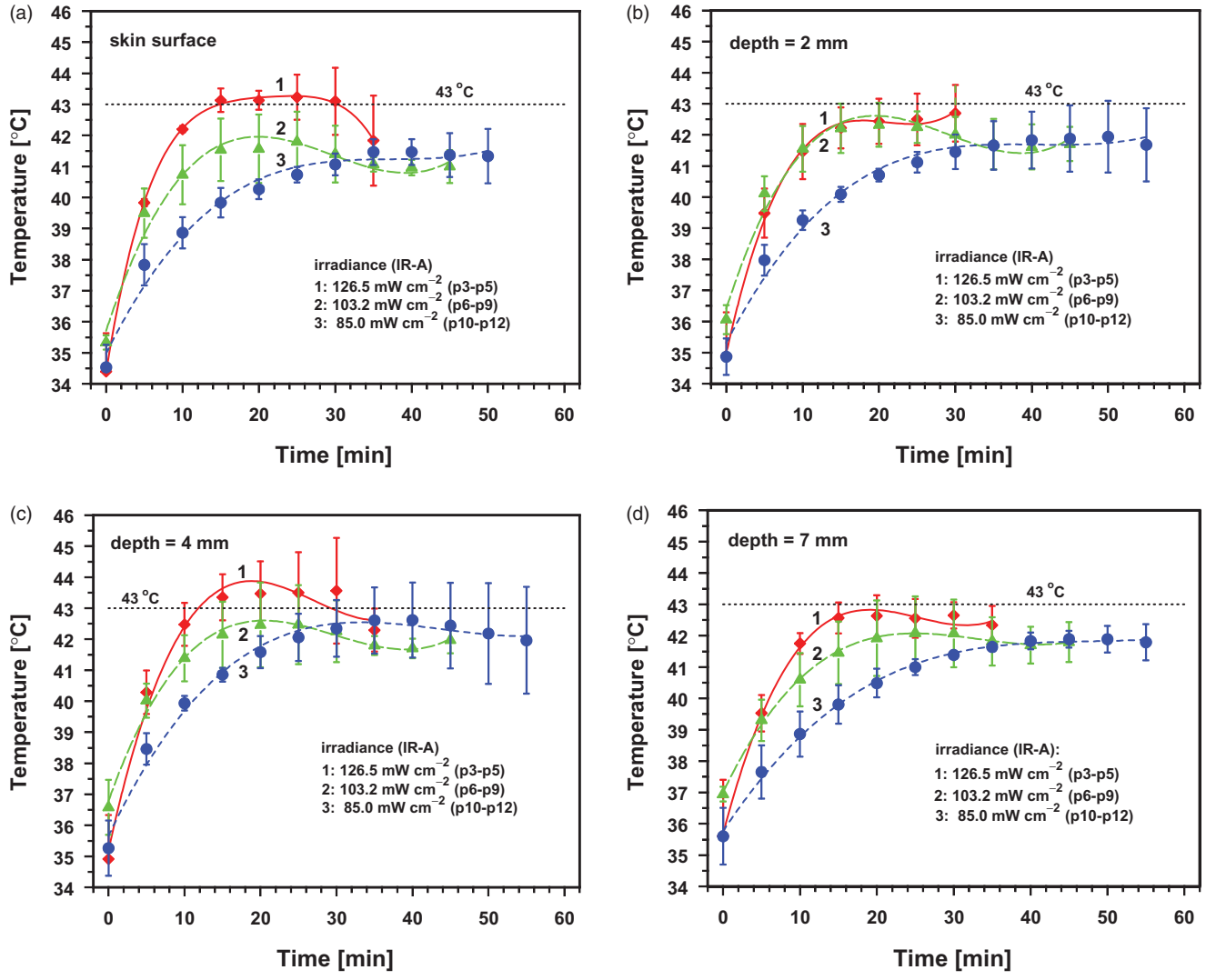

Figure 6. Mean values and standard deviations of temperatures during wIRA-irradiation with incident irradiances (IR-A) of 126.5 mW cm^{-2} (group 1, p3–p5), 103.2 mW cm^{-2} (group 2, p6–p9) and 85.0 mW cm^{-2} (group 3, p10–p12) as a function of irradiation time at the skin surface (a) and at tissue depths between 2 and 7 mm (b–d). Broken line: upper temperature limit in 'sensitizing' hyperthermia (43 °C).

maxima at the skin surface and in the tissue were up to about 1.8 K and were negligible in two cases (Figure 11b).

3.2.8. wIRA irradiation times to reach therapeutically relevant tissue temperatures

Depending on the indication, therapeutic tissue temperatures between 39 °C and 43 °C are needed. As marked by solid symbols in Figure 9a and b, temperatures of 39 °C and 40 °C were achieved in all piglets between the skin surface and depths of 20 mm for all irradiances applied. In all animals, temperatures between 41 °C and 43 °C were observed, but in certain layers only (solid symbols), or in single piglets (open symbols) (Figure 9c–e).wIRA-irradiation times to reach certain target temperatures in the tissue depended on irradiance and heat transport from the skin to deeper tissue layers. Shortest times were recorded for skin heating due to heat accumulation. The latter is caused by (a) decreased heat transport from the skin to the fat layer (as an insulating barrier), and (b) by heat loss in the upper skin layer due to heat transition from the skin surface to the environment (by thermal radiation and conductive heat exchange with the air) reducing the temperature gradient between the skin surface and deeper skin layers. Both effects prolonged the wIRA-irradiation times to reach the required tissue temperatures or even prevented therapeutically relevant temperatures in some piglets (see Figure 9a–e). Table 6 provides respective data of the exposure times to generate temperatures between 39 °C and 43 °C at the skin surface as well as in the skin at a depth of 4 mm, at the lower part of the fat layer at a depth of 10 mm, and in the muscle at depths of 16 and 20 mm.

3.2.9. Persistence of increased tissue temperatures after termination of wIRA-irradiation

Effective tissue heating can be achieved by pulsed infrared irradiation controlled by simultaneous monitoring of the skin surface temperature [27]. In combined therapeutic concepts, infrared heating of the tissue is used to increase the efficacy of subsequent therapeutic measures, as described for recurrent breast cancer by Notter et al. [23,24]. In both cases,

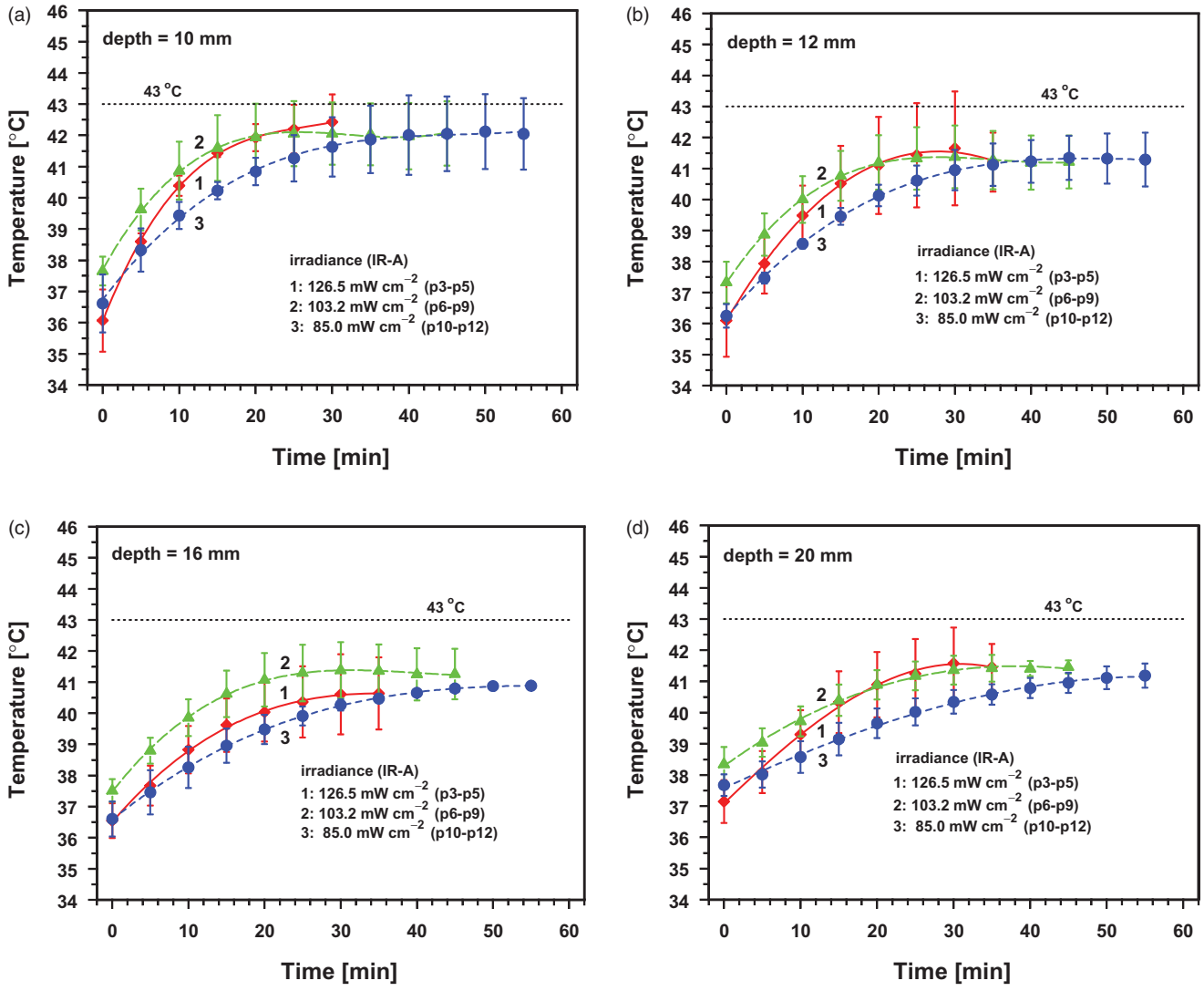

Figure 7. Mean values and standard deviations of temperatures during wIRA-irradiation with incident irradiances (IR-A) of 126.5 mW cm^{-2} (group 1, p3–p5), 103.2 mW cm^{-2} (group 2, p6–p9) and 85.0 mW cm^{-2} (group 3, p10–p12) as a function of irradiation time at tissue depths between 10 and 20 mm (a–d). Broken line: upper temperature limit in 'sensitizing' hyperthermia (43 °C).

information about the kinetics of the temperature decline in the tissue after finishing wIRA-irradiation is needed (a) for safety reasons to prevent tissue overheating that may be caused by too fast changes between irradiation and break (pulse rate), and (b) to retain a required hyperthermia status of the tissue between preheating and the following treatment (e.g., re-RT [23,24]). Thus, considering a stop of wIRA-irradiation as soon as skin surface temperature reaches 43 °C and continuation of irradiation after reaching 42 °C again, model calculations performed by Dombrovsky et al. [51] for human skin resulted in a temperature increase in the skin of about 0.2 K (as compared to skin surface temperature under the condition of thermal steady state and before the onset of thermal regulation processes).

Some examples of the temperature decreases measured at the skin surface and in the tissue after wIRA-irradiation are presented in Figure 4a–d. If a certain post-irradiation hyperthermia level (PIHL) is required, decay times and tissue depths have to be considered. Considering a minimal hyperthermia level of 39 °C, decay times to reach the baseline values again were dominated by individual heat dissipation which resulted in an extreme variation of the data. However, mean decay times increased with increasing depth as expected, and were up to about 8 min at the skin surface, up to about 15 min in the skin, 5–28 min in the fat layer, and about 42 min in the muscle at a depth of 20 mm (see Figure 10).

For higher PIHL values the decay times decreased significantly and showed means of less than 10 min in the tissue for PIHL = 40 °C and less than 5 min for PIHL = 43 °C. However, in only a few piglets, tissues were heated up to temperatures >41 °C at depths below the fat layer (see Figures 6–9). The mean decay times to reach reliable PIHLs between 40 °C and 42 °C increased slightly with increasing irradiance after wIRA-irradiation. This was caused by higher mean skin surface and tissue temperatures at the end of irradiation. (For more details see related Figures S12a–d in the Supplemental Material)

3.2.10. Skin reddening upon wIRA-irradiation

Skin reddening may indicate an intensification of the peripheral blood flow rate for thermoregulation, blood pooling

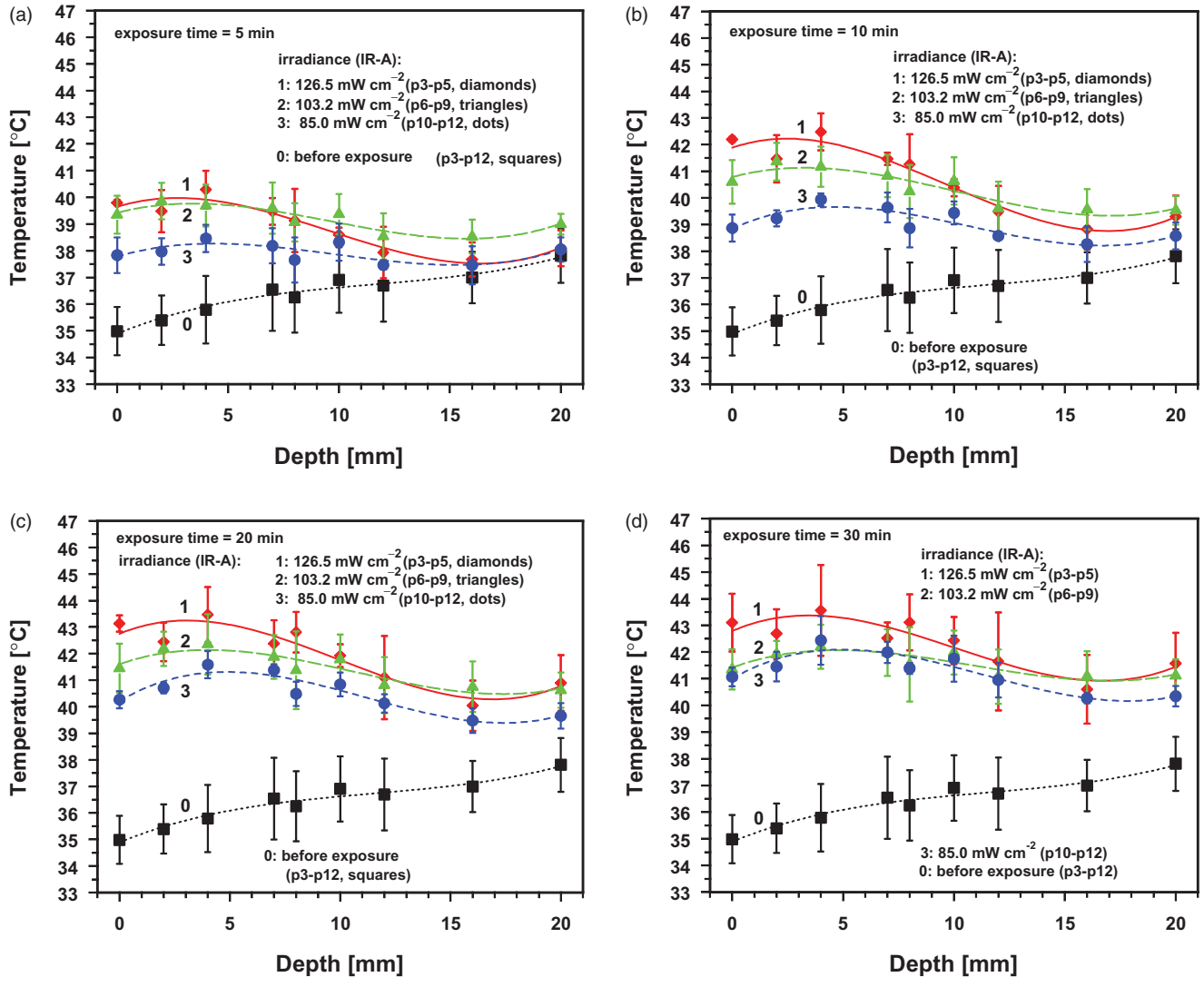

Figure 8. Mean values and standard deviations of temperatures before wIRA-irradiation (group 0, p3–p12), and after irradiation times of 5 min (a), 10 min (b), 20 min (c) and 30 min (d) with an incident irradiance (IR-A) of 126.5 mW cm^{-2} (group 1, p3–p5), 103.2 mW cm^{-2} (group 2, p6–p9) and 85.0 mW cm^{-2} (group 3, p10–p12) as a function of tissue depth.

and/or early thermal skin damage. It was observed in five piglets after wIRA-irradiation. To quantify the induced skin reddening, the colorimetric erythema index (CEI) was calculated according to COLIPA [52] using the equation:

$$\mathrm{CEI} = a^*(t_e) - a^*(t_0) \quad (3)$$

where $a^*(t_0)$ and $a^*(t_e)$ denote the red-green components in the CIE color space before ($t = t_0$) and immediately after wIRA-irradiation ($t = t_e$).

As shown in Table 7, calculated data of the symptomatic animals were limited to values of CIE $\leq$ 2.9, indicating only a small degree of redness. In two cases the redness was homogeneous, in one piglet reticular-dendritically speckled. In two additional cases it changed from a reticular-dendritic to a homogeneous distribution and disappeared completely within the cooling-down period after exposure for all five piglets (see Table 7). Thus, these results can be interpreted as a hint for (a) a probably minor role of an increase in peripheral blood flow for thermoregulation in piglets compared to humans, and (b) the absence of thermal skin damages upon wIRA-treatment [53].

4. Conclusions

4.1. Temperature at the skin surface and in the tissue during and following wIRA-irradiation

(a) The temperature rise in porcine skin and subcutis depends on irradiance, exposure time, tissue depth and thermally effective factors such as body core temperature, thicknesses of skin and fat layer and effectiveness of the local thermoregulation.

(b) Abnormal high body core temperature and a thick subcutaneous fat layer may promote overheating of the tissue including burns during exposure even with irradiances well-tolerated by normal individuals.

(c) Due to the limitation of the differences between the temperature maxima in the tissue and the corresponding skin surface temperature up to 1–2 K, skin surface temperature measurements considering these differences can be

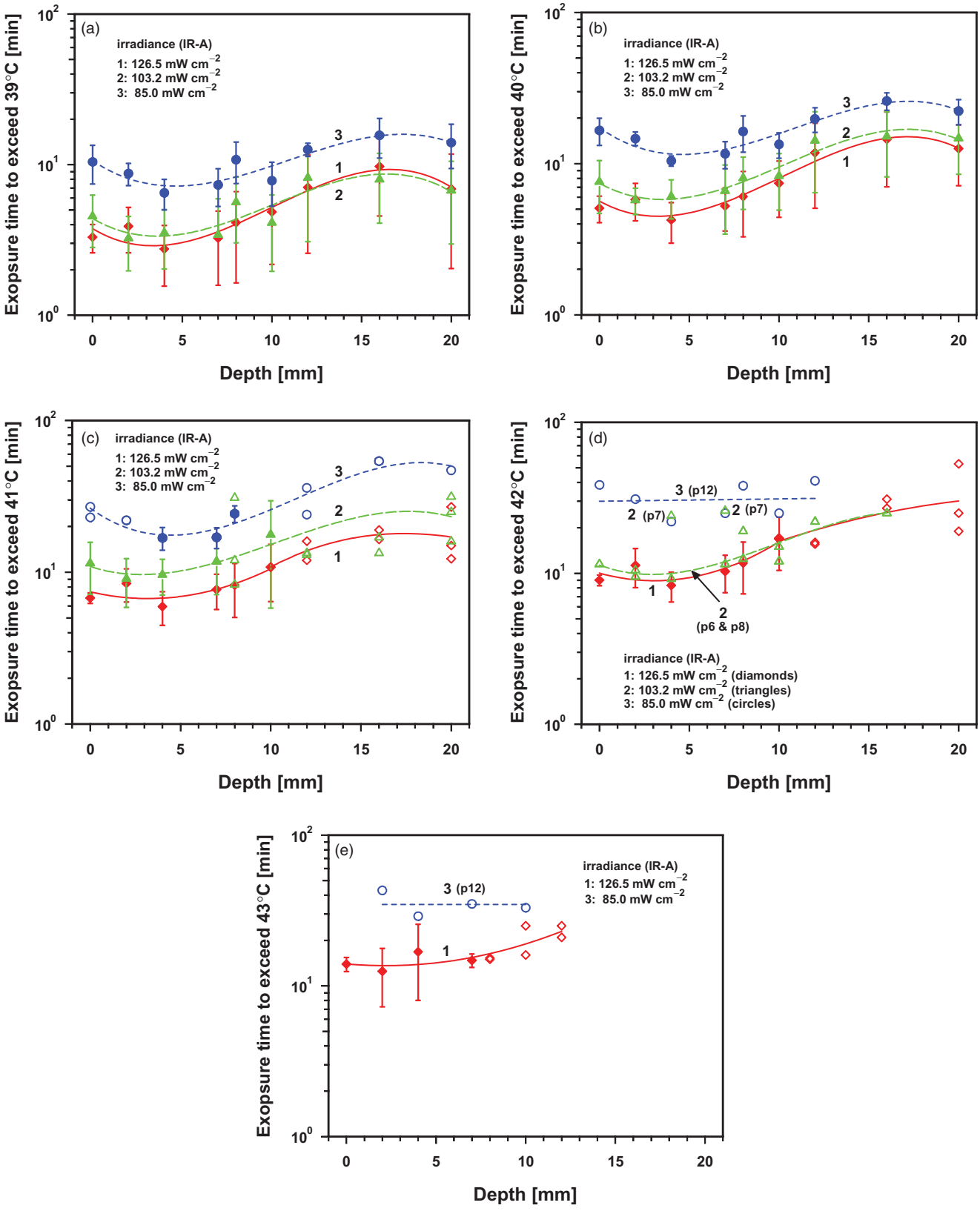

Figure 9. wIRA-irradiation times needed to reach target temperatures of 39 °C (a), 40 °C (b), 41 °C (c), 42 °C (d) and 43 °C (e) as a function of tissue depth during wIRA exposure with 126.5 mW cm^{-2} (p3–p5, group 1, red diamonds and lines), 103.2 mW cm^{-2} (p6–p9, group 2, green triangles and lines) and 85.0 mW cm^{-2} (p10–p12, group 3, blue dots and lines). Means and standard deviations of all piglets of the group reaching the target temperature (solid symbols). Individual data: only one or a few piglets of the group reaching the target temperature (open symbols).

used in almost all cases for an estimation of the maximum tissue temperature during hyperthermia in order to prevent tissue overheating and acute thermal damages of the tissue as discussed in Section 3.2.6. Further recommendations to prevent thermal injury and burning are: (i) reduction of irradiance, (ii) reduction of irradiation time to a therapeutically needed minimum and (iii) the use of pulsed exposure controlled by simultaneous skin surface temperature measurement.

(d) Since temperature decay times after wIRA-treatment depend on tissue depth and decrease with increasing PIHL, they exhibit significant inter-individual changes. The time between heating and the start of the following treatment should be shorter than the shortest decay time measured to retain the heating state of the tissue needed for therapeutic efficacy of a combination therapy. Shortest decay times for PIHL = 39 °C were up to about 5 min, for PIHL = 40–42 °C up to about 1 min, and can only be determined in single cases for PIHL = 43 °C. Therefore, the risk of overheating tissues during pulsed wIRA-irradiation is low, but cannot be excluded and requires further experimental investigations.

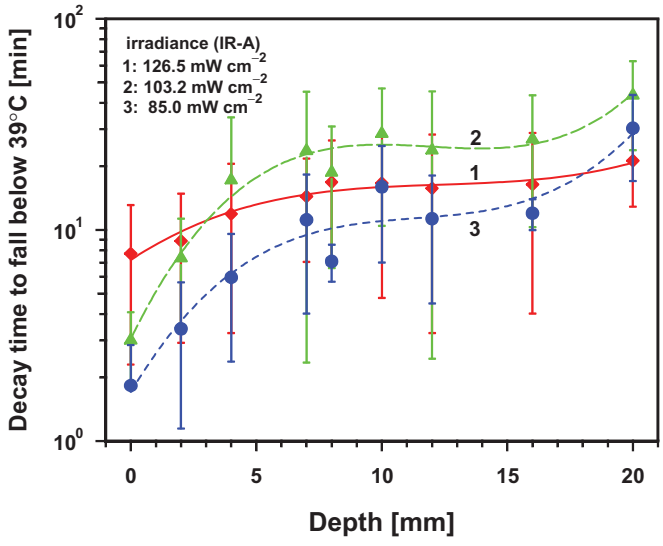

Figure 10. Time to reach the post-irradiation hyperthermia level (PIHL) of 39 °C after wIRA exposure with 126.5 mW cm^{-2} (p3–p5, group 1, red diamonds and line), 103.2 mW cm^{-2} (p6–p9, group 2, green triangles and line) and 85.0 mW cm^{-2} (p10–p12, group 3, blue dots and line).

4.2. Therapeutic options using wIRA-irradiation times to reach thermal steady state

(a) Within mean irradiation times of 30 min, temperatures ≥40 °C at depths up to 20 mm were reliably reached even with an incident irradiance of only 85.0 mW cm^{-2} (IR-A). Considering this fact, an effective thermal inactivation of the *M. ulcerans* and other thermosensitive pathogens as noted by Gazel and Yilmaz [28] can be assured. Therefore, wIRA-hyperthermia is suitable for the treatment of Buruli ulcer infections as an effective and more convenient alternative (contact free heating) compared to conventional methods. It is also recommended to determine the efficacy of wIRA-hyperthermia for thermal inactivation of other microbial pathogens by exceeding their minimum inactivation temperature in the infected tissue (e.g., *Chlamydia trachomatis, M. leprae,* periodontal pathogens). This could be a promising new therapeutic approach to prevent possible problems due to antibiotic resistances and to surgical inaccessibility.

(b) Target temperatures ≥42 °C can be generated with an irradiance of 126.5 mW cm^{-2} up to a depth of 8 mm (see Figure S13d, curve 1 in the Supplemental Material). However,

Table 5. Depth of heated tissue after 30 min of wIRA-irradiation as a function of (i) irradiance (IR-A) for different mean temperatures (T_{mean}) according to Figure 8(d), of (ii) the temperatures at the lower limit of standard deviation ($T_{\sigma l}$) according to Equation (1) and Figure S13d, and of (iii) the temperatures at the lower confidence limit of the mean using a significance level of 5% (T_{lcl}) according to Equation (2) and Figure S14d (Figures S13 and S14 are shown in the Supplemental Material).

Reference temperature	Depth of heated tissue (mm) after 30 min of wIRA-irradiation with		
	126.5 mW cm^{-2}	103.2 mW cm^{-2}	85.0 mW cm^{-2}
T_{mean}			
≥39 °C	>20	>20	>20
≥40 °C	>20	>20	>20
≥41 °C	20	20	12
≥42 °C	11	10	10
≥43 °C	8	Not reached	Not reached
$T_{\sigma l}$			
≥39 °C	>20	>20	>20
≥40 °C	20	20	20
≥41 °C	12	10	10
≥42 °C	8	Not reached	Not reached
≥43 °C	Not reached	Not reached	Not reached
T_{lcl}			
≥39 °C	20	20	20
≥40 °C	10	10	9
≥41 °C	8	8	8
≥42 °C	Not reached	Not reached	Not reached
≥43 °C	Not reached	Not reached	Not reached

Table 4. Means and standard deviations (σ) of maximum temperature (T_{max}) and thermal steady-state temperatures (SST) at the skin surface and at different tissue depths upon wIRA-irradiation.

	Maximum (T_{max}) and thermal steady-state temperature (SST) (°C) upon wIRA-irradiation							
	p2 (single values)		Group 1 (p3–p5) (means ± σ)		Group 2 (p6–p9) (means ± σ)		Group 3 (p10–p12) (means ± σ)	
Layer (depth)	T_{max}	SST	T_{max}	SST	T_{max}	SST	T_{max}	SST
Surface (0 mm)	44.2	No	43.2 (±0.7)	No	41.8 (±1.0)	41.0 (±0.6)	41.5 (±0.4)	41.3 (±0.9)
Skin (4 mm)	45.2	No	43.6 (±1.7)	42.2 (±0.7)	42.5 (±0.3)	41.7 (±0.3)	42.6 (±1.0)	42.2 (±1.6)
Fat layer (7 mm)	45.3	No	42.6 (±0.7)	42.3 (±0.6)	42.1 (±1.0)	41.7 (±0.6)	41.9 (±0.3)	41.8 (±0.6)
Fat layer (10 mm)	44.8	No	42.4 (±0.9)	No	42.1 (±1.0)	42.1 (±1.0)	42.1 (±1.2)	42.1 (±1.1)
Subcutis (12 mm)	43.7	No	41.7 (±1.8)	41.2 (±0.9)	41.4 (±1.0)	41.2 (±0.9)	41.3 (±0.8)	41.3 (±0.8)
Subcutis (20 mm)	42.4	No	41.5 (±1.0)	41.5 (±0.7)	41.4 (±0.9)	41.4 (±0.2)	41.1 (±0.4)	41.1 (±0.4)

Data are presented for piglets p3–p5 [group 1, exposed to 126.5 mW cm^{-2} (IR-A)], for piglets p6–p9 [group 2, exposed to 103.2 mW cm^{-2} (IR-A)] and for piglets p10–p12 [group 3, exposed to 85.0 mW cm^{-2} (IR-A)]. Single values for piglet p2 are shown for comparison.

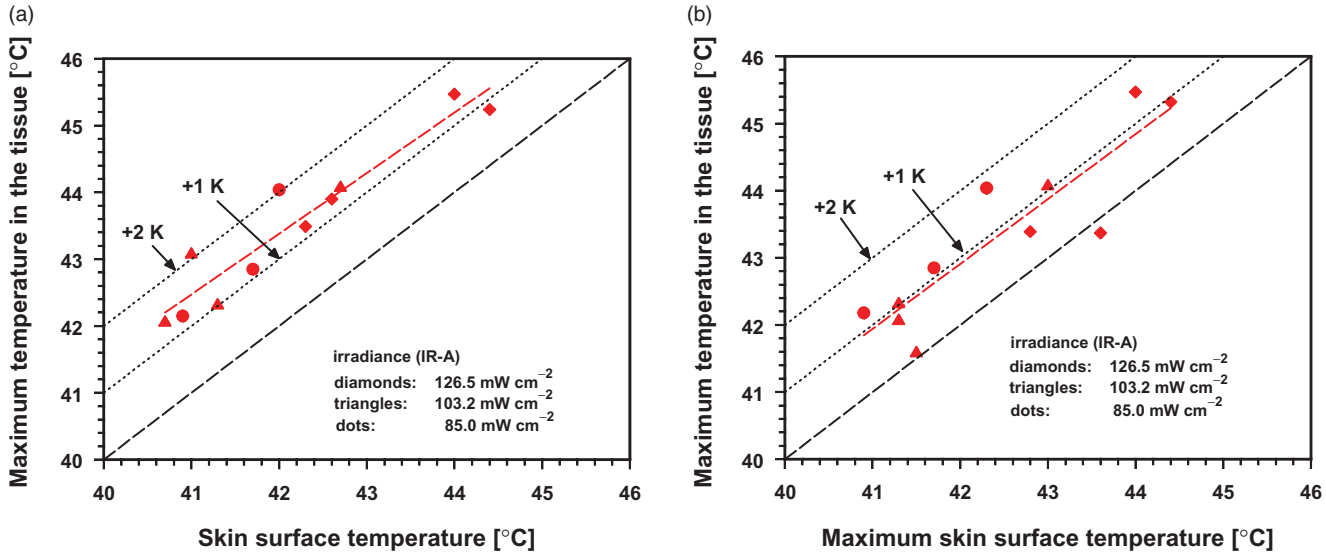

Figure 11. Maximum tissue temperature as a function of synchronously measured skin surface temperature (a) and maximum temperature at the skin surface during wIRA-irradiation (b). Diamonds: piglets 2–5, exposed to 126.5 mW cm^{-2} (IR-A); triangles: piglets 6–9, exposed to 103.2 mW cm^{-2}; dots: piglets 10–12, exposed to 85.0 mW cm^{-2}. Piglets p2 and p5 showed maximum tissue temperatures above 45 °C.

Table 6. Exposure times for different wIRA irradiances (IR-A) to reach target temperatures between 39 °C and 43 °C at the skin surface (depth = 0 mm), in the skin at a depth of 4 mm, at the lower part of the fat layer at 10 mm and in the muscle at depths of 16 and 20 mm.

Target temperature (°C)	Group (irradiance) (mW cm^{-2})	Exposure time to reach target temperature (min) at different depths (complete group: mean ± σ, incomplete group: range)				
		0 mm	4 mm	10 mm	16 mm	20 mm
39	1 (126.5)	3.3 ± 0.7	2.8 ± 1.2	4.9 ± 2.7	9.7 ± 5.2	6.9 ± 4.9
	2 (103.2)	4.6 ± 1.7	3.5 ± 1.5	4.1 ± 2.2	8.0 ± 3.9	6.8 ± 3.8
	3 (85.0)	10.4 ± 3.0	6.5 ± 1.5	7.9 ± 2.5	15.7 ± 4.6	14.0 ± 4.6
40	1 (126.5)	5.1 ± 1.0	4.3 ± 1.3	7.4 ± 3.0	14.5 ± 7.5	12.6 ± 5.5
	2 (103.2)	7.6 ± 2.9	6.1 ± 1.8	8.3 ± 3.4	15.2 ± 7.0	14.8 ± 6.2
	3 (85.0)	16.6 ± 3.4	10.5 ± 0.8	13.4 ± 2.6	26.0 ± 3.6	25.3 ± 5.5
41	1 (126.5)	6.8 ± 0.5	6.0 ± 1.5	10.8 ± 4.2	16.5 ± 19.0	12.3 – 27.0
	2 (103.2)	11.5 ± 4.3	9.6 ± 2.6	10.8 ± 4.4	13.4 ± 17.0	16.0 – 31.5
	3 (85.0)	23.0 – 27.0	16.8 ± 2.8	Not reached	54.0	36.0 – 47.0
42	1 (126.5)	9.0 ± 0.7	8.3 ± 1.9	17.0 ± 6.6	27.0 – 31.0	19.0 – 53.0
	2 (103.2)	11.5	9.2 – 24.0	12.0 – 15.0	25.0	Not reached
	3 (85.0)	38.5	22.0	25.0	Not reached	Not reached
43	1 (126.5)	13.0 ± 1.5	16.8 ± 8.8	16.0 – 25.0	Not reached	Not reached
	2 (103.2)	Not reached	Not reached	Not reached	Not reached	Not reached
	3 (85.0)	Not reached	29.0	33.0	Not reached	Not reached

Values are means and standard deviations (σ) for all piglets of the group reaching the target temperature. Individual data: only one piglet reached the target temperature.

Table 7. a^*-data before ($t = t_0$), immediately after wIRA-irradiation ($t = t_e$) and after the cooling-down period (t_c), duration of the cooling-down period ($\Delta t_c = t_c - t_e$).

Piglet	$a^*(t_0)$	$a^*(t_e)$	CEI	$a^*(t_d)$	Δt_c (min)	Visual redness
p2	1.3	1.5	0.2	1.5	–	No
p3	1.1	1.1	0.0	1.1	–	No
p4	1.2	2.3	1.1	1.3	60	Homogeneous
p5	1.6	3.0	1.4	1.8	60	Reticular-dendritic
p6	1.4	1.1	−0.2	1.1	–	No
p7	2.2	3.4	1.2	1.6	55	At first reticular-dendritic,
p8	1.8	4.7	2.9	2.4	55	homogeneous thereafter
p9	3.5	2.9	−0.6	–	–	No
p10	2.4	1.7	−0.7	–	–	No
p11	2.9	3.1	0.2	1.9	–	No
p12	1.6	4.1	2.5	1.4	20	Homogeneous

Calculated values for the colorimetric erythema index (CEI) and characterization of visual redness.

two piglets reached 42 °C up to depths of 16 mm after 31 min and up to 43 °C up to depths of 10 mm after 25 min. In the other two piglets of this group, increased heat dissipation reduced the temperatures to less than 42 °C at tissue layers deeper than 10 mm and to less than 43 °C at depths deeper than 4 mm. Thus, to ensure target temperatures ≥42 °C (as occasionally used in hyperthermia of superficial cancers) at depths deeper than 8 mm [26,54], individually

adjusted measures to compensate heat dissipation are needed. These include (i) higher incident irradiances and (ii) extended exposure times. In any case, heating has to be controlled by invasive temperature measurements or temperature estimation as described in Section 4.1.c.

4.3. Relevance of the experimental data for wIRA-hyperthermia of humans

(a) In order to assess the transferability of the results described to humans, the following facts must be taken into consideration: (i) in contrast to humans, pigs are unable to cool their skin by sweating; (ii) normal values of the body core and the blood temperature are about 1 K higher than in humans; (iii) skin and fat layers in pigs are thicker than in humans and (iv) an increase in peripheral blood flow is an essential part of the thermoregulation in healthy humans, which results in skin reddening to intensify heat dissipation. This phenomenon was observed in five piglets only immediately after the end of wIRA-treatment. Moreover, it is known that general anesthesia can cause hypothermia in patients, typically by 1–2 K [55]. However, as verified by the continuous body core temperature recordings (see Table 1, Figures 4a–d, curves 10, and in the Supplemental Figures S1a–S11a, curves 10), this phenomenon did not occur in the piglets during the experiments. Therefore, further investigations based on direct in vivo measurements in humans are needed to adapt the data described above to the requirements in the human situation.

Disclosure statement

The authors declare that the research was conducted in the absence of any commercial of financial relationship that could be constructed as a potential conflict of interest.

Ethics statement

Ethical approval for the experiments was obtained from Veterinäramt Kanton Zürich (Ref.: ZH180/15). Date of approval: 9 February 2016.

Funding

This study was supported by the Dr. med. h.c. Erwin Braun Foundation, Basel, Switzerland (X.S., H.P. and W.M.). Peter Vaupel is a long-standing board member *ad honorem* of the Dr. med. h.c. Erwin Braun Foundation.

ORCID

Gerd Pluschke http://orcid.org/0000-0003-1957-2925

References

[1] Rzeznik J. Die Technik zur loko-regionalen Wärmetherapie mit wassergefilterter Infrarot-A-Strahlung. In: Vaupel P, Krüger W, editors. Wärmetherapie mit wassergefilterter Infrarot-A-Strahlung. Grundlagen und Anwendungsmöglichkeiten. Stuttgart (Germany): Hippokrates-Verlag; 1995. p. 29–46.

[2] Piazena H, Kelleher DK. Effects of infrared-A irradiation on skin: discrepancies in published data highlight the need for an exact consideration of physical and photobiological laws and appropriate experimental setups. Photochem Photobiol. 2010;86:687–705.

[3] Piazena H, Meffert H, Uebelhack R. Spectral remittance and transmittance of visible and of infrared-A radiation in human skin – comparison between *in vivo* measurements and model calculations. Photochem Photobiol. 2017;93:1449–1461.

[4] Stoll AM, Greene LC. Relationship between pain and tissue damage due to thermal radiation. J Appl Physiol. 1959;14:373–382.

[5] DIN 33403-2. Klima am Arbeitsplatz und in der Arbeitsumgebung - Teil 2: Einfluss des Klimas auf den Wärmehaushalt des Menschen. Berlin (Germany): Beuth Verlag; 2000.

[6] Piazena H, Meffert H, Uebelhack R. Physical and photobiological basics for prophylactic and therapeutic application of infrared radiation. Akt Dermatol. 2014;40:335–339.

[7] Vaupel P, Stofft E. Water-filtered infrared-A radiation in comparison to conventional infrared radiation or fango-paraffin packs: temperature profiles during local hyperthermia. In: Vaupel P, Krüger W, editors. Wärmetherapie mit wassergefilterter Infrarot-A-Strahlung. Grundlagen und Anwendungsmöglichkeiten. Stuttgart (Germany): Hippokrates-Verlag; 1995. p. 135–147.

[8] Hoffmann G. Clinical applications of water-filtered infrared-A (wIRA) - a review. Phys Med Rehab Kuror. 2017;27:265–274.

[9] Heckel M. Ganzkörper-Hyperthermie und Fiebertherapie - Grundlagen und Praxis. Stuttgart (Germany): Hippokrates-Verlag; 1990.

[10] Vaupel P, Stohrer M, Krüger W, et al. Localized hyperthermia in superficial tumors using water-filtered infrared-A- radiation: evaluation of temperature distribution and tissue oxygenation in subcutaneous rat tumors. Strahlenther Onkol. 1991;167:353–354.

[11] Vaupel P, Kelleher DK, Krüger W. Water-filtered infrared-A radiation: a novel technique to heat superficial tumors . Strahlenther Onkol. 1992;168:633–639.

[12] Vaupel P, Kelleher DK, Krüger W. Wassergefilterte Infrarot-A-Strahlung: Eine neue Technik zur lokalen Hyperthermie oberflächlich liegender Tumoren. In: Vaupel P, Krüger W, editors. Wärmetherapie mit wassergefilterter Infrarot-A-Strahlung. Stuttgart (Germany): Hippokrates-Verlag; 1992. p. 57–62.

[13] Kelleher DK, Engel T, Vaupel P. Changes in microregional perfusion, oxygenation, ATP and lactate distribution in subcutaneous rat tumours upon water-filtered IR-A hyperthermia. Int J Hyperthermia. 1995;11:241–255.

[14] von Ardenne M. Systemische Krebs-Mehrschritt-Therapie – Hyperthermie und Hyperglykämie als Therapiebasis. Grundlagen, Konzeption, Technik, Klinik. Stuttgart (Germany): Hippokrates-Verlag; 1997.

[15] Thews O, Li Y, Kelleher DK. Microcirculatory functions, tissue oxygenation, microregional redox status and ATP distribution in tumors upon localized infrared-A-hyperthermia at 42 °C. Adv Exp Med Biol. 2003;530:237–247.

[16] Kelleher DK, Thews O, Rzeznik J. Water-filtered infrared-A radiation: a novel technique for localized hyperthermia in combination with bacteriochlorophyll-based photodynamic therapy. Int J Hyperthermia. 1999;15:467–474.

[17] Kelleher DK, Thews O, Scherz A, et al. Combined hyperthermia and chlorophyll-based photodynamic therapy: tumour growth and metabolic microenvironment. Br J Cancer. 2003;89:2333–2339.

[18] Kelleher DK, Bastian J, Thews O, et al. Enhanced effects of aminolaevulinic acid-based photodynamic therapy through local hyperthermia in rat tumours. Br J Cancer. 2003;89:405–411.

[19] Zywietz F. Infrarot-A-Hyperthermie als strahlensensibilisierendes Agens bei Bestrahlung oberflächennah liegender Tumoren: Tierexperimentelle Untersuchungen. In: Vaupel P, Krüger W, editors. Wärmetherapie mit wassergefilterter Infrarot-A-Strahlung. Stuttgart (Germany): Hippokrates-Verlag; 1995. p. 113–126.

[20] Morita K, Zywietz F, Kakinuma K, et al. Efficacy of doxorubicin thermosensitive liposomes (40 degrees C) and local hyperthermia on rat rhabdomyosarcoma. Oncol Rep. 2008;20:365–372.

[21] Seegenschmiedt MH. Erfahrungen mit einem Infrarot-A-Hyperthermie-Projektor mit Wasserfilter zur lokal-perkutanen Hyperthermie kombiniert mit Radiotherapie bei oberflächennahen Tumoren. In: Vaupel P, Krüger W, editors, Wärmetherapie mit wassergefilterter Infrarotstrahlung. Stuttgart (Germany): Hippokrates-Verlag; 1992. p. 63–76.
[22] Seegenschmiedt MH, Klautke G, Walther E, et al. [Water-filtered infrared-A-hyperthermia combined with radiotherapy in advanced and recurrent tumors. Initial results of a multicenter phase I-II study]. Strahlenther Onkol. 1996;172:475–484.
[23] Notter M, Piazena H, Vaupel P. Hypofractionated re-irradiation of large-sized recurrent breast cancer with thermography-controlled, contact-free water-filtered infra-red-A hyperthermia: a retrospective study of 73 patients. Int J Hyperthermia. 2017;33:227–236.
[24] Notter M, Münch K, Vaupel P. Re-Irradiation and wIRA-hyperthermia for superficial widespread breast cancer recurrences: an update. 31st Annual Meeting of the European Society for Hyperthermic Oncology (ESHO), Athens; 2017.
[25] Vaupel P, Piazena H, Müller W, et al. Biophysical and photobiological basics of water-filtered infrared-A hyperthermia of superficial tumors. Int J Hyperthermia. 2018;35:26–36.
[26] Trefna HD, Creeze H, Schmidt M, et al. Quality assurance guidelines for superficial hyperthermia clinical trials: I. Clinical requirements. Int J Hyperthermia. 2017;33:471–482.
[27] Dobsicek Trefna H, Crezee J, Schmidt M, et al. Quality assurance guidelines for superficial hyperthermia clinical trials: II. Technical requirements for heating devices. Strahlenther Onkol. 2017;193:351–366.
[28] Gazel D, Yilmaz M. Are infectious diseases and microbiology new fields for thermal therapy research?. Int J Hyperthermia. 2018;34:918–924.
[29] WHO. 2012. Treatment of *Mycobacterium ulcerans* disease (Buruli ulcer) – guidance for health workers. Available from: apps.who.int/iris/bitstream/10665/77771/1/9789241503402_eng.pdf.
[30] O'Brian DP, Jenkin G, Buntine PP, et al. Treatment and prevention of *mycobacterium ulcerans* infection (Buruli ulcer) in Australia: guideline update. Med J Aust. 2014;200:267–270.
[31] Meyers WM, Shelly WM, Connor DH. Heat treatment of *mycobacterium ulcerans* infections without surgical excision. Am J Trop Med Hyg. 1974;23:924–929.
[32] Junghanss T, Um Boock A, Vogel M, et al. Phase change material for thermotherapy of Buruli Ulcer: a prospective observational single centre proof-of-principle trial. PLOS Negl Trop Dis. 2009;3:e380.
[33] WHO. 2018. Available from: www.who.int/buruli/en/.
[34] Asiedu K, Scherpbier R, Raviglione M. 2000. *Buruli ulcer - Mycobacterium ulcerans* infection. Available from: http://www.who.int/iris/handle/10665/66164.
[35] Ruf MT, Bolz M, Vogel M, et al. Spatial distribution of *Mycobacterium ulcerans* in Buruli ulcer lesions: Implications for laboratory diagnostics. PLOS Negl Trop Dis. 2016;10:e0004767. pntd.0004767.
[36] Kuratli J, Pesch T, Marti H, et al. Water-filtered infrared-A and visible light (wIRA/VIS) irradiation reduces *Chlamydia trachomatis* infectivity independent of targeted cytokine inhibition. Front Microbiol. 2018;9:2757.
[37] Ibelli T, Templeton S, Levi-Polyachenko N. Progress on utilizing hyperthermia for mitigating bacterial infections. Int J Hyperthermia. 2018;34:144–156.
[38] Mackowiak PA. Direct effects of hyperthermia on pathogenic microorganisms: teleologic implications with regard to fever. Rev Infect Dis. 1981;3:508–520.
[39] Chopra R, Levi-Polyachenko N, Smeltzer MS. Introduction to the special issue on thermal therapy and infectious diseases. Int J Hyperthermia. 2018;34:133–134.
[40] Marti H, Koschwanez M, Pesch T, et al. Water-filtered infrared-A irradiation in combination with visible light inhibits acute chlamydial infection. Plos One. 2014;9:e102239.
[41] Marti H, Blenn C, Borel N. The contribution of temperature, exposure intensity and visible light to the inhibitory effect of irradiation on acute chlamydial infection. J Photochem Photobiol B. 2015;153:324–333.
[42] Onorini D, Donati M, Marti H, et al. The influence of centrifugation and incubation temperature on various veterinary and human chlamydial species. Vet Microbiol. 2019;233:11–20.
[43] Rahn C, Marti H, Frohns A, et al. Water-filtered infrared-A reduces chlamydial infectivity in vitro without causing ex vivo eye damage in pig and mouse models. J Photochem Photobiol B. 2016;165:340–350.
[44] Moritz A, Henriques F. Studies of thermal injury. II. The relative importance of time and surface temperature in the causation of cutaneous burns. Am J Pathol. 1947;23:695–720.
[45] Dewhirst MW, Viglianti BL, Lora-Michiels M, et al. Thermal dose requirement for tissue effect: experimental and clinical findings. Proc SPIE Int Soc Opt Eng. 2003;4954:37.
[46] Viglianti BL, Dewhirst MW, Abraham JP, et al. Rationalization of thermal injury quantification methods: application to skin burns. Burns. 2014;40:896–902.
[47] Bolz M, Ruggli N, Borel N, et al. Local cellular immune responses and pathogenesis of Buruli ulcer lesions in the experimental *Mycobacterium ulcerans* pig infection model. PLOS Negl Trop Dis. 2016;10:e0004678. pntd.0004678.
[48] Sutter E. Schutz vor optischer Strahlung. Laserstrahlung, inkohärente Strahlung, Sonnenstrahlung. Normenreihe DIN EN 60825 (VDE 0837). VDE-Schriftenreihe 104. Berlin (Germany): VDE-Verlag; 2002.
[49] CIE. CIE colorimetry – part 4: 1976 L^* a^* b^* colour space. Vienna (Austria): CIE; 1976.
[50] Gaus W, Muche R. Medizinische Statistik. Stuttgart (Germany): Schattauer Verlag; 2014.
[51] Dombrovsky LA, Timchenko V, Pathak C, et al. Radiative heating of superficial human tissues with the use of water-filtered infrared-A radiation: a computational modeling. Int J Heat Mass Transf. 2015;85:311–320.
[52] COLIPA Guideline. Guideline for the colorimetric determination of skin colour typing and prediction of the minimal erythemal dose (MED) without UV exposure. Brussels (Belgium): COLIPA; 2007.
[53] Meffert H, Piazena H, Kolde G. The infrared erythemas - from infrared-A and -C erythema to Erythema ab Igne. Akt Dermatol. 2008;34:119–123.
[54] Dewhirst MW, Vujaskovic Z, Jones E, et al. Re-setting the biologic rationale for thermal therapy. Int J Hyperthermia. 2005;21:779–790.
[55] Sessler D. Perioperative thermoregulation and heat balance. Lancet. 2016 Jan;387:2655–2664.